OPTICAL CHARACTERIZATION OF ERBIUM DOPED III-NITRIDES PREPARED BY METALORGANIC MOLECULAR BEAM EPITAXY

U. Hömmerich*[,+], J. T. Seo*, Myo Thaik*, J. D. MacKenzie**, C. R. Abernathy**, S.J. Pearton**, R.G. Wilson†, J. M. Zavada‡

*Hampton University, Department of Physics, Research Center for Optical Physics, Hampton, VA 23668

**University of Florida, Department of Materials Science and Engineering, Gainesville, FL 32611

†Consultant, Stevenson Ranch, CA 91381

‡U.S. Army European Research Office, London, UK, NW1 5

[+] E-mail: hommeric@gprc.hamptonu.edu

ABSTRACT

We are currently engaged in a systematic study of the optical properties of Er doped III-nitrides prepared by metalorganic molecular beam epitaxy (MOMBE). Under below-gap excitation it was observed that GaN: Er samples with [O]~10^{20} cm^{-3} and [C]~10^{21} cm^{-3} luminesce at 1540 nm with an intensity of more than two orders of magnitude greater than samples with low oxygen and carbon concentrations (< 10^{19} cm^{-3}). Associated with the different oxygen and carbon concentrations were different thermal quenching behaviors and below-gap absorption bands. Interestingly, for above-gap excitation only small differences in absolute Er^{3+} PL intensity and quenching behavior were observed for samples of varying O and C content. Initial lifetime studies were performed and showed a rather unusual short decay time of ~100 μs at room temperature. In order to gain more insight in the Er^{3+} PL, a comparison of the integrated PL intensity and lifetime was performed for the temperature range 15-500K. The result reveals that the Er^{3+} PL quenches above room temperature due to the onset of non-radiative decay and the reduction in excitation efficiency. All samples were also investigated for visible luminescence. Red luminescence was observed from GaN: Er on sapphire substrates under below-gap excitation.

INTRODUCTION

Rare earth doped semiconductors have been studies for more than a decade because of the possibility to develop compact and efficient electroluminescence devices.[1,2,3,4] Trivalent Erbium ions (Er^{3+}) are of special interest because they exhibit an atomic-like transition at 1540nm, which corresponds to the low-loss window of silica-based optical fibers. Electroluminescence devices based on Er doped Si and GaAs were reported, however, their efficiency was too low for practical applications.[3,4] An important step forward in the field of Er doped semiconductors was the observation that the room-temperature Er^{3+} photoluminescence (PL) intensity strongly depends on the bandgap of the host materials. It was found that for larger bandgap energy, there is less detrimental temperature quenching of Er^{3+} PL occurring.[5,6] Therefore, doping Er^{3+} ions into wide gap semiconductors is a promising approach to overcome the thermal quenching of Er^{3+} PL. Consequently, current research efforts focus on studying Er^{3+} doped into wide bandgap semiconductors such as SiC and GaN.[7,8] First results on the observation of 1.54 μm photoluminescence from Er implanted GaN and AlN were reported by Wilson et al.[9] Subsequently, other research groups reported results of photoluminescence, cathodoluminescence, and electroluminescence (EL) studies of Er implanted GaN. [10,11,12,13] The goal for practical device applications is to incorporate Er^{3+} ions during epitaxial growth. Doping during growth has several advantages over ion implantation including the absence of implantation damage, unlimited layer thickness, and a more homogenous doping profile. In-situ

https://doi.org/10.1557/S1092578300003653 Published online by Cambridge University Press

Er doping of AlN using metalorganic molecular beam expitaxy (MOMBE) was first reported by MacKenzie et al. in 1996.[14] This work was followed by the first demonstration of in-situ Er doping of GaN.[15] Recently, Hansen et al. reported results of in-situ doped GaN: Er prepared by hydride vapor phase growth.[16] Visible PL and EL from GaN: Er grown by molecular beam epitaxy have been reported.[17,18] Even though encouraging strong Er^{3+} PL results were obtained, initial infrared electroluminescence studies of GaN: Er have shown rather poor efficiencies.[19,20] In order to optimize the material preparation for developing more efficient 1.54 μm devices, it is crucial to understand the incorporation and excitation mechanisms of Er^{3+} ions in III-Nitrides. More specifically, it will be important to identify the Er^{3+} sites that are excited efficiently through electrical injection of electron-hole pairs and to optimize their concentration in the GaN host.[12] In this paper we present new spectroscopic results focusing on the 1.54 μm PL from MOMBE grown Er doped GaN. Results of temperature dependent PL intensity, lifetime, and excitation studies will be shown and discussed for samples with varying oxygen and carbon content. In addition, we will also report some initial results on visible luminescence studies.

EXPERIMENTAL PROCEDURES

The Er doped GaN films were grown by MOMBE in an INTEVAC Gas Source Gen II on In-mounted (100) Si or (0001) Sapphire substrates. The GaN films were preceded by a low temperature AlN buffer (T_g=425 °C). A 0.2 μm undoped GaN spacer was deposited prior to the growth of GaN: Er. Triethylgallium (TEGa), Dimethylethylamine alane (DMEAA), and thermally-evaporated 8N Ga metal provided the group III fluxes. A shuttered effusion oven with 4N Er was used for solid source doping. Reactive nitrogen species were provided by a SVT radio frequency plasma source. Due to the incorporation of carbon and oxygen from residual ether in TEGa, the C and O background observed in TEGa derived GaN were $\sim 10^{21} cm^{-3}$ and $\sim 10^{20} cm^{-3}$, respectively, as determined by SIMS measurements. GaN grown using thermally-evaporated 8N pure Ga as the group III source had oxygen and carbon backgrounds of less than $10^{19} cm^{-3}$.[21]

PL measurements were performed using either the broad-band visible (457-514nm) or uv (333.6-363.8nm) outputs of an argon-ion laser for excitation. The luminescence spectra were recorded using a 1-m monochromator equipped with a liquid-nitrogen cooled Ge detector. Visible PL studies employed a thermo-electric cooled photomultiplier tube. The signal was processed using lock-in technique. The samples were cooled on the cold-finger of a two-stage closed-cycle refrigerator. High temperature PL studies were carried out using a homemade heating element, which had a temperature accuracy of ±5°C. Luminescence lifetime data were taken with a fast response Ge detector and averaged using a digitizing oscilloscope. PLE studies were carried out using an argon pumped dye laser or and a Nd: YAG/Optical Parametric Oscillator system.

RESULTS AND DISCUSSION

a) Er^{3+} PL intensity and spectra

Figure 1 shows the room-temperature, infrared PL spectra of Er doped GaN on Al_2O_3 prepared by MOMBE. No significant spectral differences were observed for Er doped GaN on Sapphire or Si substrates. For comparison, the Er^{3+} PL spectra of AlN: Er (MOMBE) and Er implanted GaN are also shown in figure 1.[9,14] All samples were excited with the 363-366.8nm UV output of an Argon-Ion laser. UV excitation was chosen to simulate carrier-mediated Er^{3+} excitation as in GaN: Er electroluminescence devices. All samples showed characteristic Er^{3+} PL centered at 1.54 μm, which can be assigned to the intra-4f Er^{3+} transition $^4I_{13/2}$--->$^4I_{15/2}$. The Er^{3+}

https://doi.org/10.1557/S1092578300003653 Published online by Cambridge University Press

PL spectra from in-situ Er doped GaN and AlN are very similar. They exhibit nearly featureless spectra (25-35nm @FWHM) suggesting a homogenous distribution of Er sites as typically observed from Er doped glasses.[22,23] Er peaks located at 1.517µm, 1.540µm, 1.548µm, and 1.555 µm are either due to Stark splittings and/or multiple Er sites. The overall spectral width of the Er^{3+} PL from Er implanted GaN was significantly larger (100nm@FWHM) than that observed from Er doped GaN and AlN. Moreover, Er implanted GaN exhibits a more sharply structured Er^{3+} PL than the in-situ Er doped III-Nitride samples. Based on previously published data [9,10,11,12,13], the more complex and broad Er^{3+} PL seems to be characteristic for Er implanted GaN samples and is due to a combination of different Er sites and Stark splittings of Er ions in low symmetry sites. For example, Kim et al. identified up to 4 Er sites in Er implanted GaN grown by MOCVD.[12] The authors demonstrated that it was possible to selectively excite these four sites by three different below-gap absorption processes and through direct intra-4f excitation. Important for future device development was the observation that only a small fraction of incorporated Er^{3+} ions are excitable through carrier-mediated processes.[24] Time-resolved PL studies of in-situ Er doped AlN (MOMBE) have indicated the existence of at least two different classes of Er^{3+} sites with distinct lifetime and excitation schemes.[25] These results underline that it is crucial to identify the incorporation and excitation mechanism of Er^{3+} in different sites in order to optimize the material preparation for device applications.

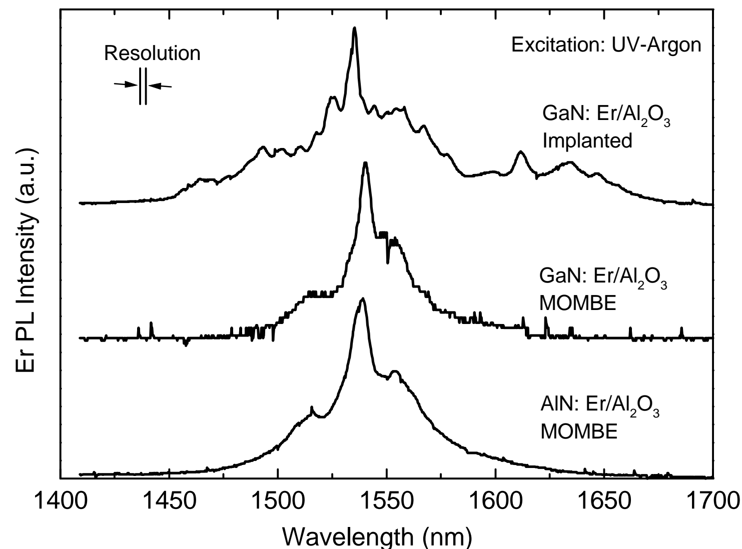

Figure 1: Room-temperature Er^{3+} PL spectra of Er implanted GaN and in-situ Er doped GaN and AlN.

Figure 2 depicts a comparison of the absolute Er^{3+} PL intensities of GaN: Er (MOMBE) for below and above-gap excitation at room-temperature. Under below-gap excitation, GaN: Er (TEGa) with high oxygen and carbon background ([O]~$10^{20}cm^{-3}$, [C]~$10^{21}cm^{-3}$) showed an Er^{3+} PL peak intensity two orders of magnitude larger than GaN: Er (Ga) with low O and C backgrounds (<$10^{19}cm^{-3}$). It is interesting to note that also GaN: Er/Si showed strong 1.54µm PL at room temperature, which makes this material attractive for integration with Si based optoelectronics.[21] Drastic improvements of the absolute Er^{3+} PL intensity have been observed for Er and oxygen codoped Si and GaAs. The enhanced 1.54µm PL was attributed to an increased concentration of optically active Er^{3+} ions and a more efficient Er^{3+} PL excitation.[26,27,28,29,30] Our results for below-gap Er^{3+} excitation in GaN suggest that the incorporation of O and C introduces

https://doi.org/10.1557/S1092578300003653 Published online by Cambridge University Press

beneficial mid-gap states that provide efficient energy transfer pathways for Er^{3+} in GaN. Support for this idea was obtained from photoluminescence excitation (PLE) studies shown in figure 3. In PLE the effectiveness of stimulating 1.54 μm Er^{3+} PL is measured as a function of excitation wavelength. The PLE spectra of GaN: Er/Si (TEGa) reveal that the incorporation of high O and C backgrounds leads to a broad PLE band extending over the entire visible region (~400-800 nm). The GaN: Er (Ga) sample with low C and O content did not show this broad PLE band, but direct intra-4f Er transitions (see e.g. ~525nm). Therefore, the visible output from an Argon-Ion laser leads to a significantly more efficient excitation of Er^{3+} in GaN:Er/Si (TEGa) than in GaN: Er/Si (Ga).

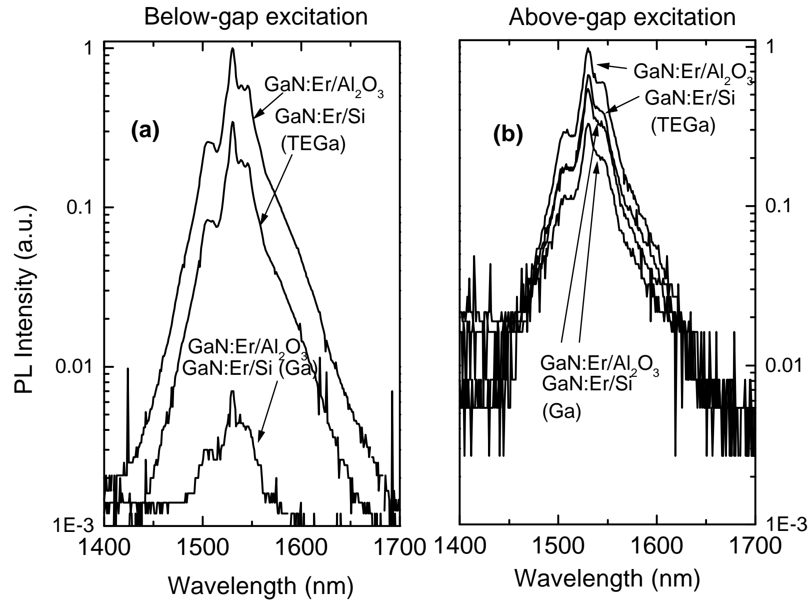

Figure 2: Comparison of Er^{3+} PL intensity from Er doped GaN (MOMBE) for a) below-gap and (b) above-gap excitation (300K).

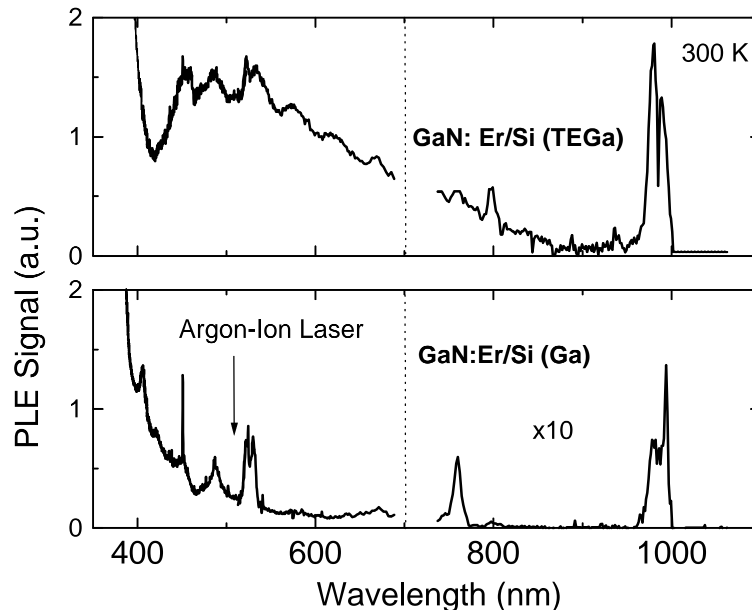

Figure 3: PLE of GaN: Er/Si samples with varying oxygen and carbon content. The incorporation of high oxygen and carbon backgrounds (upper graph) leads to a broad Er^{3+} excitation band covering the entire visible region.

https://doi.org/10.1557/S1092578300003653 Published online by Cambridge University Press

Under above-gap excitation (figure 2b) all GaN: Er (MOMBE) samples showed a greatly reduced Er^{3+} PL intensity relative to below-gap excitation, independent of carbon and oxygen concentration. A similar PL reduction was reported for Er implanted GaN.[31] It is somewhat surprising that under above-gap excitation the Er^{3+} PL intensities of samples with high oxygen and carbon backgrounds is only roughly twice as strong as the Er^{3+} PL observed from low O and C contents. These observations suggest that either only a fraction of optically active Er^{3+} ions are excited and/or the excitation efficiency is reduced under above-excitation. Moreover, it also indicates that high oxygen and carbon concentrations do not necessary lead to an enhanced luminescence for carrier-mediated Er^{3+} excitation. More work is necessary to address this issue in more detail.

b) Er PL quenching and lifetime

Figure 4 shows the integrated Er^{3+} PL intensity of Er doped GaN samples for the temperature range from 15-500K. The Er^{3+} PL was excited either with the broad-band visible (Fig. 4a) or uv (Fig. 4b) outputs of an Argon ion laser corresponding to below and above-gap Er^{3+} excitation. Under below-gap excitation a significantly different Er^{3+} PL quenching behavior was observed for samples with varying O and C contents (see Figure 4a). As was previously observed for Er and oxygen codoped Si and GaAs, GaN: Er samples with high O and C concentrations showed a significantly reduced Er^{3+} PL quenching compared to samples with low C and O backgrounds.[26,27,28,29,30] Between 15K and room-temperature samples with high O and C backgrounds showed Er^{3+} PL quenching of only ~20%, whereas the 1.54μm luminescence from low O and C concentration samples decreased by ~90% over the same temperature range. At higher temperatures also the O and C rich samples showed an enhanced Er^{3+} PL quenching and the luminescence decreased to roughly 10% of their low temperature value at 500K. Under above-gap excitation the situation was different. As shown in Fig. 4(b) hardly any difference in Er^{3+} PL quenching behavior was observed for samples with varying oxygen/carbon content. As mentioned above, the oxygen and carbon concentration does not greatly effect the carrier-mediated Er^{3+} excitation. Up to room temperature the Er^{3+} PL decreased for all four samples by less than 50% relative to its low temperature value. When heating the samples above room temperature, we observed a steady decrease of the Er^{3+} PL with increasing temperature. At 550 K, the Er^{3+} PL from all samples had decreased by nearly 90% of its low temperature value.

To gain more insight in the observed Er^{3+} PL quenching, we performed initial luminescence lifetime studies on the two oxygen and carbon rich samples, GaN: Er/Si (TEGa) and GaN:Er/Sapphire (TEGa). These samples showed the strongest Er^{3+} PL signal, which allowed us to carry out lifetime studies for the entire range 15-500 K. It was observed that the Er^{3+} PL decay curves were non-exponential which provides further support for the existence of a wide distribution of Er^{3+} sites. To describe the luminescence decay an average lifetime $<\tau>$ was used:

$$<t>=\frac{\int I(t)tdt}{\int I(t)dt} \tag{1}$$

where I(t) is the luminescence decay curve and t is the time.[32,33] The low temperature lifetime of both samples was found to be ~130μs and decreased to ~100μs at room temperature. At 500K the lifetime had shortened to ~50μs. These lifetimes are significantly shorter than previously reported lifetimes for Er implanted GaN, which were in the order of 1-2ms.[10,16] It is possible that the short lifetimes are due to a higher oscillator strength of Er^{3+} transitions in MOMBE grown samples compared to Er implanted GaN. In order to confirm this explanation direct absorption measurements of intra-4 Er transitions are necessary. It is also conceivable that the Er^{3+} lifetimes

https://doi.org/10.1557/S1092578300003653 Published online by Cambridge University Press

are shortened due intra-4f non-radiative decay or cooperative processes such as upconversion or energy migration.[34] Power dependent lifetime studies, however, did not show any change in lifetime with increasing excitation density suggesting that the later processes are not dominant in GaN:Er.

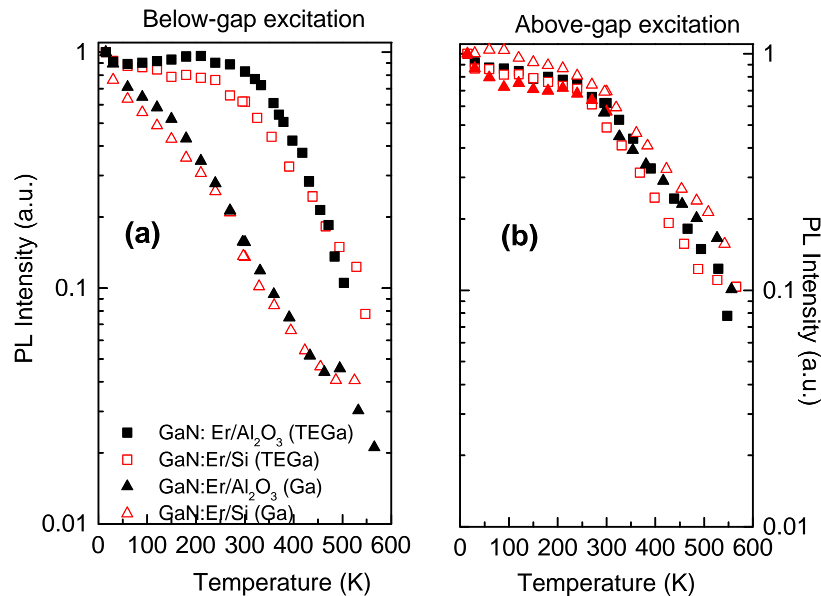

Figure 4: Temperature dependence of the integrated PL intensity from in-situ Er doped GaN for above and below gap excitation.

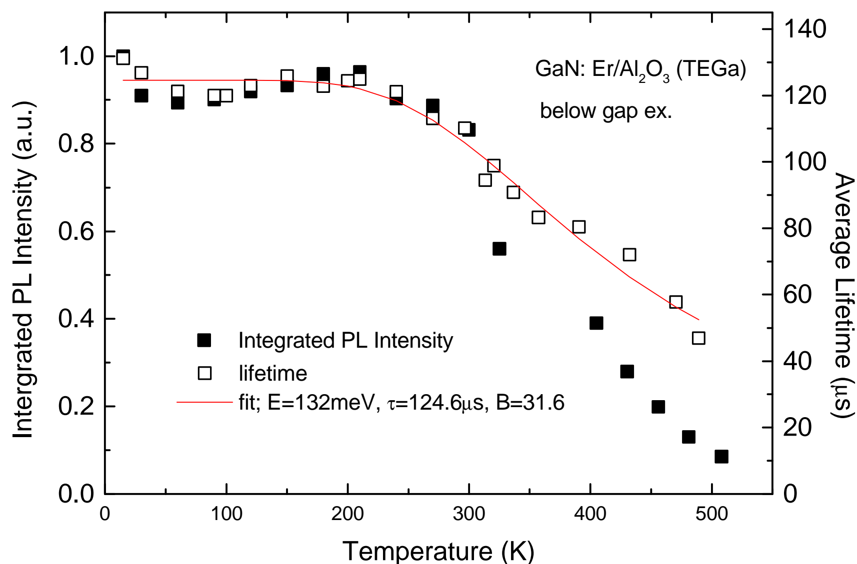

Figure 5: Comparison of the temperature dependence of Er^{3+} intergrated PL and lifetime for in-situ Er doped GaN.

It is instructive to compare the temperature dependence of PL intensity and lifetime as shown in figure 5. In the following discussion it is assumed that the Er^{3+} PL intensity is proportional to the number (or concentration) of excited Er ion (N_{Er}^{*}) and the radiative decay rate (w_{rad}). Under steady state condition and low pump power intensities the Er^{3+} PL signal can be written as:

https://doi.org/10.1557/S1092578300003653 Published online by Cambridge University Press

$$I_{PL} = C \cdot \frac{I_p}{hc} \cdot \lambda_p \cdot \sigma_{ex} \cdot N_{tot} \cdot w_{rad} \cdot \tau \tag{2}$$

where C is a constant, I_p is the pump intensity, λ_p is the pump wavelength, σ_{ex} is the excitation cross-section defined as the product of pump efficiency and absorption cross-section, N_{tot} is the total Er concentration, w_{rad} is the radiative decay rate, and τ is the luminescence lifetime. Under the assumption that the radiative decay rate and total Er concentrations are temperature independent, the Er^{3+} PL quenching at higher temperatures can be explained by either the onset of nonradiative deexcitation processes reducing the Er^{3+} lifetime and/or by a decrease of the excitation efficiency.

The comparison of the temperature dependent Er^{3+} PL intensity and lifetime enables one to separate the above mentioned Er^{3+} PL quenching mechanism. As can be inferred from figure 5, the Er^{3+} lifetime follows the change in integrated PL intensity very closely up to room temperature. This means that between 15 and 300K the small decrease in Er^{3+} PL intensity is due to nonradiative decay. Above room-temperature the lifetime changes less than the integrated Er^{3+} PL intensity. This suggests that Er^{3+} PL quenching occurring above room temperature is not only due nonradiative deexcitation, but also due to a reduction in excitation efficiency. Nearly the same Er^{3+} PL intensity and lifetime behavior was observed for GaN:Er/Si (not shown). Similar to other Er doped semiconductor systems, we assume that the excited Er ion can decay either through emission of a 1.54 µm photon or through non-radiative energy transfer processes to the host (also referred to as "backtransfer" [28,35]). It is further assumed that internal Er^{3+} quantum efficiency does not change with temperature. The change in lifetime is then described by a thermally activated nonradiative decay process, which is controlled by Boltzmann's law:

$$\frac{1}{\tau} = \frac{1}{\tau_{rad}}\left(1 + B \cdot \exp\left(-\frac{E}{kT}\right)\right) \tag{3}$$

where τ_{rad} is the radiative lifetime, E is the thermal activation or threshold energy for non-radiative decay, and B is a constant. Fitting equation 3 to the lifetime data shown in figure 5 gives the following parameter values: τ_{rad}= 124.6µs, B=31.6, and an activation energy E=132meV. The fit result suggests the existence of a defect-related level close to Er^{3+}, which acts as a particular effective channel for nonradiative energy transfer between Er^{3+} and the host. The deexcitation of Er ions through some mid-gap level has been discussed before for Er doped Si and GaAs. In the backtransfer model as proposed by Takahei et al.[28], the existence of an Er-related level provides the possibility of energy backtransfer where excited Er ions transfer an excited carrier back to the defect level followed by a thermalization into the conduction band. This model for the deactivation of excited Er^{3+} ions may also be relevant for GaN:Er, however, no experimental evidence for an Er-related defect level has yet been reported. A more detailed comparison of the Er^{3+} lifetimes of GaN: Er samples with varying oxygen and carbon content is in progress and promises to provide deeper insight in the Er excitation and deexcitation mechanisms.

c) visible PL from GaN: Er

Very recently green luminescence was observed from GaN: Er grown by solid source molecular beam epitaxy under above-gap excitation.[36] Narrow lines centered at 537nm and 558nm were identified to be due to the intra-4f Er transitions $^2H_{11/2}\rightarrow{}^4I_{15/2}$ and $^4S_{3/2}\rightarrow{}^4I_{15/2}$. Subsequently the same authors reported green electroluminescence from Er doped GaN Schottky

https://doi.org/10.1557/S1092578300003653 Published online by Cambridge University Press

barrier diodes.[37] In figure 6 we show the visible PL spectra of GaN: Er/Sapphire prepared by MOMBE. We observed no green emission lines from any of the investigated samples under below (488nm) or above-gap (325nm) excitation. Interestingly, however, for below-gap excitation we observed a broad red luminescence band, which showed sharp structure at around 665 nm and 690 nm. This emission was not found for the GaN: Er/Si samples. Preliminary studies indicated that the peaks at 665 nm and 690 nm had lifetimes in the millisecond range. The peak at 665 nm is assigned to the $^4F_{9/2} \rightarrow ^4I_{15/2}$ transition of Er^{3+} ions, whereas the origin of the 690 nm peak is not yet know. The data suggest that the 690 nm line is a pure electronic transition (no-phonon line) accompanied by a vibronic sideband at around 720 nm. A more detailed study is currently being undertaken to identify the origin of the red luminescence from GaN:Er/Sapphire.

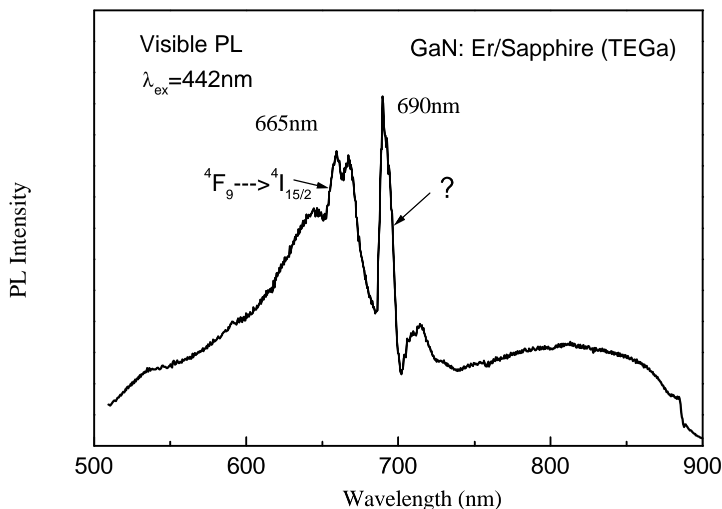

Figure 6: Visible PL spectrum of GaN: Er/Sapphire for below-gap excitation at room-temperature.

SUMMARY

We presented new results on the 1.54 µm luminescence properties of GaN: Er grown by MOMBE. It was observed that high oxygen and carbon concentrations (~10^{20} cm^{-3}) enhance the 1.54µm Er^{3+} PL intensity and reduce the Er^{3+} PL quenching under below-gap excitation. Moreover, PLE studies revealed that oxygen/carbon introduces a broad below-gap PLE band, which provides an efficient pathway for Er^{3+} excitation. A direct comparison of the temperature dependence of Er^{3+} PL intensity and lifetime suggests that both nonradiative decay and a decrease in excitation efficiency reduce the Er^{3+} PL. Under above-gap excitation the absolute Er^{3+} PL intensity from all samples was greatly reduced and only a weak PL dependence on the oxygen and carbon concentration was observed. The weak above-gap Er^{3+} PL suggests that the efficiency of electroluminescence devices (forward biased LED's) based on currently available materials will be rather low. More materials engineering will be necessary to optimize the 1.54µm Er^{3+} PL from GaN: Er. Initial results of visible luminescence studies were also presented. It was found that only under below-gap excitation GaN:Er on sapphire emits red luminescence peaking at 665 and 690 nm. The 665 nm line was assigned to an intra-4f Er^{3+} transition, whereas

https://doi.org/10.1557/S1092578300003653 Published online by Cambridge University Press

the origin of the 690 nm line is not yet known. More detailed studies on the luminescence properties of GaN: Er are in progress in will be presented in a forthcoming paper.

ACKNOWLEDGMENTS

We would like to thank George Ofori-Boudu and Jakeithia Preajan for the help with some PL experiments. The authors from Hampton University acknowledge financial support by NASA through Grant NCC-1-251 and the Army Research Office through Grants DAAH04-96-1-0089 and DAAG55-98-1-0112. The work at the University of Florida was supported by ARO grant DAAH04-96-1-0089.

REFERENCES

[1] R. L. Bell, J. Appl. Phys. Comm. **34**, 1563 (1963).

[2] H. Ennen, U. Kaufmann, G. S. Pomrenke, J. Schneider, J. Windschif, and A. Axmann, J. Crystal Growth **64**, 165 (1983).

[3] G. S. Pomrenke, P. B. Klein, and D. W. Langer, Rare Earth Doped Semiconductors, Material Research Society Symposium Proceedings, Vol. 301, Material Research Society, Pittsburg, 1993.

[4] S. Coffa, A. Polman, and R.N. Schwartz, Rare Earth doped Semiconductors II, Materials Research Society Symposium Proceedings, Vol. 422, Material Research Society, Pittsburgh, PA, 1996.

[5] P. N. Favennec, H.L. Haridon, M. Salvi, D. Moutonnet, and Y. Le Guillou, Electr. Lett. **25**, 718 (1989).

[6] A.J. Neuhalfen and B.W. Wessels, Appl. Phys. Lett. **60**, 2657 (1992).

[7] W. J. Choyke, R. P. Devaty, L. L. Clemen, M. Yoganathan, G. Pensl, and Ch. Hässler, Appl. Phys. Lett. 65, 1668 (1994).

[8] J. M. Zavada and D. Zhang, Solid-State Electronics, Vol. **38**, No.7, 1285 (1995).

[9] R. G. Wilson, R. N. Schwartz, C. R. Abernathy, S. J. Pearton, N. Newman, M. Rubin, T. Fu, and J. M. Zavada, Appl. Phys. Lett. **65**, 992 (1994).

[10] C.H. Qui, M. W. Leksono, J. I. Pankove, J. T. Torvik, R. J. Feuerstein, and F. Namavar, Appl. Phys. Lett. **66**, 562 (1995).

[11] E. Silkowski, Y.K. Yeo, R. L. Hengehold, B. Goldenberg, and G. S. Pomrenke, MRS Proceedings, Vol. **422**, 69 (1996).

[12] S. Kim, S. J. Rhee, D. A. Turnbull, E. E. Reuter, X. Li, J. J. Coleman, and S. G. Bishop, Appl. Phys. Lett. **71**, 231 (1997).

[13] Myo Thaik, U. Hömmerich, R. N. Schwartz, R. G. Wilson, and J.M. Zavada, Appl. Phys. Lett. **71**, 2641 (1997).

[14] J. D. MacKenzie, C. R. Abernathy, S. J. Pearton, U. Hömmerich, X. Wu, R. N. Schwartz, R. G. Wilson, J. M. Zavada, Appl. Phys. Lett. **69**, 2083 (1996).

[15] J. D. MacKenzie, C. R. Abernathy, S. J. Pearton, U. Hömmerich, X. Wu, R. N. Schwartz, R. G. Wilson, J. M. Zavada, J. Cryst. Growth **175/176**, 84 (1997).

[16] D.M. Hansen, R. Zhang, N. R. Perkins, S. Safvi, L. Zhang, K.L. Bray, and T. F. Kuech, Appl. Phys. Lett **72**, 1244 (1998).

[17] A. J. Steckl and R. Birkhahn, Appl. Phys. Lett. **73**, 1701 (1998).

[18] A. J. Steckl, M. Garter, R. Birkhahn, and J. Scofield, Appl. Phys. Lett. **73**, 2450, (1998).

[19] J. T. Torvik, R. J. Feuerstein, C. H. Qui, J. I. Pankove, and F. Namavar, J. Appl. Phys. **69** 2098 (1996).

https://doi.org/10.1557/S1092578300003653 Published online by Cambridge University Press

[20] H. Shen, J. Pamulapati, J. D. Mackenzie, F. Ren, C. R. Abernathy, and J. M. Zavada, MRS Fall Meeting 1998, paper G11.5.
[21] J. D. MacKenzie, C. R. Abernathy, S. J. Pearton, U. Hömmerich, J. T. Seo, R. G. Wilson, and J. M. Zavada, Appl. Phys. Lett. **72**, 2710 (1998).
[22] W. J. Miniscalco, J. of Lightwave Techn. **9**, 234 (1991).
[23] B. J. Ainslie, J. of Lightwave Techn. **9**, 220 (1991).
[24] S. J. Rhee, S. Kim, X. Li, J. J. Coleman, and S. G. Bishop, Mat. Res. Soc. Symp. Proc., Vol. **482**, 667 (1998).
[25] X. Wu, U. Hömmerich, J. D. MacKenzie, C. R. Abernathy, S. J. Pearton, R. N. Schwartz, R. G. Wilson, and J. M. Zavada, Appl. Phys. Lett. **70**, 2126 (1997).
[26] J. L. Benton, D.J. Eaglesham, M. Almonte, P.H. Citrin, M. A. Marcus, D.L. Adler, D. C. Jacobson, and J. M. Poate, Mat. Res. Soc. Symp. Proc., Vo. **301**, 119 (1993).
[27] S. Coffa, F. Priolo, G. Franzo, V. Bellani, A. Carnera, C. Spinella, Phys. Rev. B, **48**, 11782 (1993).
[28] K. Takahei, A. Taguchi, J. Appl. Phys. 74, 1979 (1993).
[29] J. Michel, J.L. Benton, R.F.Ferrante, D.C. Jacobson, D.J.Eaglesham, E.A. Fitzgerald, Y.H. Xie, J.M. Poate, and L.C. Kimmerling, J. Appl. Phys. **70**, 2672 (1991).
[30] S. Coffa, F. Priolo, G. Franzo, V. Bellani, A. Carnera, and C. Spinella, Mat. Res. Soc. Symp. Proc., Vol. **301**, 125, 1993.
[31] J. T. Torvik, R. J. Feuerstein, C. H. Qui, J. I. Pankove, and F. Namavar, Mat Res. Soc. Symp. Proc., Vol. **482**, 579, 1998.
[32] J. Fernandez, R. Balda, M. A. Illarramendi, G. F. Imbusch, J. Lumin. **58**, 294 (1994).
[33] L. J. Andrews, A. Lempicki, and B. C. McCollum, J. Chem. Phys. **74**, 5526 (1981).
[34] G. N. van den Hoven, Jung H. Shin, A. Polman, S. Lombardo, and S. U. Campisano, J. Appl. Phys. **78**, 2642, 1995.
[35] P. G. Kik, M. J. A de Dood, K. Kikoin and A. Polman, Appl. Phys. Lett. **70**, 1721 (1997).
[36] R. Birkhahn and A.J. Steckl, Appl. Phys. Lett. **73**, 2143 (1998).
[37] A. J. Steckl, M. Garter, R. Birkhahn, and J. Scofield, Appl. Phys. Lett. **73**, 2450, (1998).

https://doi.org/10.1557/S1092578300003653 Published online by Cambridge University Press